Orig Life Evol Biosph (2007) 37:27–45
DOI 10.1007/s11084-006-9015-8

Phosphate sorption and desorption on pyrite in primitive aqueous scenarios: Relevance of acidic → alkaline transitions

Fernando de Souza-Barros · Raphael Braz-Levigard · Yonder Ching-San Jr. · Marisa M. B. Monte · José A. P. Bonapace · Viviane Montezano · Adalberto Vieyra

Received: 14 October 2005 / Accepted: 23 March 2006 / Published online: 5 July 2006

Abstract Phosphate (P_i) sorption assays onto pyrite in media simulating primeval aquatic scenarios affected by hydrothermal emissions, reveal that acidic conditions favour P_i sorption whereas mild alkaline media – as well as those simulating sulfur oxidation to SO_4^{2-} – revert this capture process. Several mechanisms relevant to P_i availability in prebiotic eras are implicated in the modulation of these processes. Those favouring sorption are: (a) hydrophobic coating of molecules, such as acetate that could be formed in the vicinity of hydrothermal vents; (b) water and Mg^{2+} bridging in the interface mineral-aqueous media; (c) surface charge neutralization by monovalent cations (Na^+ and K^+). The increase of both the medium pH and the SO_4^{2-} trapping by the mineral interface would provoke the release of sorbed P_i due to charge polarization. Moreover it is shown that P_i self-modulates its sorption, a mechanism that depends on the abundance of SO_4^{2-} in the interface.

The relevance of the proposed mechanisms of P_i capture, release and trapping arises from the need of abundant presence of this molecule for primitive phosphorylations, since – similarly to contemporary aqueous media – inorganic phosphate concentrations in primitive seas should have been low. It is proposed that the presence of sulphide minerals with high affinity for P_i could have trapped this molecule in an efficient manner, allowing its

R B-L and Y C-S contributed equally to this work; recipients of fellowships from the Brazilian National Research Council in the PIBIC and PINC-School of Medicine programs of the Universidade Federal de Rio de Janeiro

F. de Souza-Barros (✉)
Instituto de Física, Universidade Federal do Rio de Janeiro
e-mail: fsbarros@if.ufrj.br

R. Braz-Levigard · Y. Ching-San Jr. · V. Montezano · A. Vieyra
Instituto de Biofísica Carlos Chagas Filho, Universidade Federal do Rio de Janeiro

M. M. B. Monte
Centro de Tecnologia Mineral, Ministério da Ciência e Tecnologia

J. A. P. Bonapace
Instituto de Química, Universidade Federal do Rio de Janeiro, Cidade Universitária, 21941–590 Rio de Janeiro, Brazil

concentration in specific niches. In these niches, the conditions studied in the present work would have been relevant for its availability in soluble form, especially in primitive insulated systems with pH gradients across the wall.

Keywords Iron sulfide minerals · Primitive seawater-sulfides interfaces · Acidic→alkaline transitions · Phosphate capture and release mechanisms · Modulation of phosphate availability in primitive scenarios · Phosphorylation reactions

1. Introduction

Linear polyphosphates and cyclic polyphosphates of volcanic origin could have been sources of soluble phosphate during chemical evolution (Yamagata *et al.*, 1991). It is generally accepted, however, that prebiotic aqueous environments contained very low concentrations of soluble orthophosphate (P_i) as in contemporary seawater (10^{-7}–10^{-8} M) (Keefe and Miller, 1995). One way to circumvent this low availability is to propose that insoluble phosphates, both in crystalline and amorphous states, could have participated in phosphoryl transfer reactions. Previous work have shown that: (1) pyrophosphate is formed from crystalline apatite (Miller and Parris, 1964; Vieyra *et al.*, 1995), (2) precipitated calcium orthophosphate can phosphorylate 5′-AMP to 5′-ADP (Tessis *et al.*, 1995), and (3) phosphorolytic cleavage of different phosphorylated compounds occurs with high yield on the surface of minerals (Hermes-Lima and Vieyra, 1992). Phosphorylation should have required concentration excursions of P_i in primitive aqueous environment. It is assumed in this work that a pyrite substrate would have been a favorable candidate for P_i concentration for the presence of S minerals in the Archean is widely discussed in the literature (Kasting *et al.*, 1989).

In recent work (Monte *et al.*, 2003) we have demonstrated the efficient P_i- and PP_i-trapping properties of the amorphous ferric-oxide precursor and pointed out that this mechanism - at present playing a significant role in P_i occlusion by minerals – should have been absent in anoxic abiotic scenarios. It is well known that aqueous-mineral interfaces might play a role in these trapping mechanisms. We have also considered the role of the pyrite interfacial ionic configuration in its sorption properties of 5′-AMP (Pontes-Buarque *et al.*, 2000, 2001).

Studies on the oxidation processes of sulphur compounds in water point out the dissolution of iron sulphides by oxidative processes in which water, rather than free O_2, is the primary source of oxygen in the released SO_4^{2-} product (Borda *et al.*, 2003; Usher *et al.*, 2004). In the case of pyrite in abiotic conditions, this dissolution implies the removal of its elemental constituents of the material – sulfur and iron ions – (see Figure 4 below) thus generating disordered vacancies and random sorption of a fraction of liberated iron ions (Paschka and Dzombak, 2004).

The present work investigates P_i-release mechanisms after its immobilisation onto the reactive pyrite mineral surface and modulation effects that can yield significant variations of soluble P_i concentrations in specific aqueous environments. Different aqueous models have been considered in the experimental conditions assayed: (a) primitive seawater (Snyder and Fox, 1975); (b) concentrated acetate to investigate the effect of an oxo acid that could have been formed onto the pyrite-aqueous media interface (Huber and Wächtershäuser, 1997) and modified its molecular trapping properties (Cairns-Smith, 1982; Tessis *et al.*, 1999); (c) combinations of salt solutions to enhance probing of specific effects on P_i sorption and release; and (d) deionized water to observe the effect of salt depletion upon the trapping properties of the pyrite-solution interface.

Table 1 The composition of the used artificial primitive seawater[a]

NaCl	0.42 M
KCl	8.30 mM
$CaCl_2$	7.60 mM
$SrCl_2$	0.14 mM
$MgCl_2$	23.0 mM
$MgSO_4$	26.0 mM
KBr	0.75 mM
NaF	71 μM
H_3BO_3	0.4 mM

[a] Snyder and Fox, 1975

2. Materials and methods

Pyrite head samples were extracted from charcoal mines in Tubarão (SC, Brazil). These samples were ground and washed to remove natural contaminants – mainly carbonates and silicates. Grains with size less than 53 μm were used in the described assays. Details of these procedures can be found in Tessis *et al.*, (1999). X-ray diffractograms of these grains show the dominant crystalline pyrite lines (Tessis *et al.*, 1999). Determinations of the specific area of the untreated pyrite mineral were made by the N_2-adsorption technique (BET, Brunauer *et al.*, 1938) using the BET equipment ASAP 2000 from Micromeritics Instruments Co. (Norcross, GA). These determinations yield a value $2.01 \pm 0.02\,m^2/g$ for the specific surface area of the material (head sample). The radioactive orthophosphate ($^{32}P_i$) used in this work was obtained from the Nuclear and Energy Research Institute, IPEN, (São Paulo, Brazil), high purity argon gas (99.999%) was obtained from White Martins S.A. (Rio de Janeiro, Brazil) and all other reagents were analytical reagent grade.

As mentioned above**,** the composition of artificial seawater used was that of Snyder and Fox (1975) (Table 1), modified as described in the corresponding figure captions. The starting pH values of 5.5 and 4.0 in sorption experiments were adjusted with concentrated HCl and pH 6.6 was reached by adding NaOH. In SO_4-rich media, pH was adjusted with concentrated H_2SO_4. Other aqueous media are also detailed in the figure captions. Glass-distilled water deionized by the Nanopure resins (18 MΩ cm) (Millipore Corp., Marlborough, MA) was used in the preparation of the solutions as well as pure solvent for some of the experiments .

Surface iron hydroxide was removed from the pyrite head samples by hydrofluoric acid (HF) as previously described (Tessis *et al.*, 1999). The manipulation of oxide-free pyrite samples was carried out in the oxygen-free inert atmosphere of a glove box (Cole Parmer Instruments, Vernon Hills, IL). The pyrite samples were stored under vacuum for at least 24 h.

In most of the experiments, the difference method was used to determine the amount of P_i immobilized in the pyrite-aqueous interface. The P_i concentration in the supernatant – necessary to determine the total amount of sorbed P_i – was measured using a colour-reagent solution (Fiske and SubbaRow, 1925). This solution contained iron sulphate, sulphuric acid, ammonium molybdate and water (0.5 ml) and was mixed with an equal volume of the supernatants to be analysed. After 20 min, the P_i relative content in the samples was obtained by spectrophotometry, at 660 nm, and compared with that obtained with a standard solution. As mentioned above, P_i sorption assays were performed within the pH range 4.4 to 6.6; pH 5.5 was chosen in most experiments because it characterizes current models of Hadean ocean (Martin and Russell, 2002). The sets of samples were incubated at 45 °C. $^{32}P_{i\ (s)} \leftrightarrow P_{i\ (aq)}$ exchange assays were carried out using radioactive $^{32}P_i$ for sorption, followed by a chase

with unlabelled P_i. $^{32}P_i$ activity in supernatant was determined with the liquid scintillation counter technique.

As previously described (Monte *et al.*, 1997), the determinations of the surface charge polarities of pyrite particles – dispersed in solutions with either different pH values or electrolytes – were done with a Zeta-Master type AZ103 equipment (Zeta-Meter Inc., Stanton, VA). In these assays, the pH values of the solutions were set with either HCl or NaOH.

Diffuse-Reflectance Fourier-Transform Infrared (DRIFT) spectra were recorded on a Bomem spectrometer MB102 and a deuterated triglycine sulphate (DTGS) detector with CsI windows. After removing the supernatant in inert atmosphere, fractions of the residue were packed with spectrometer-grade KBr in a mass ratio of about 1:10. The powders were then dried at 100 °C for 15 h. The final diffuse reflectance (DR) spectra are the average of one hundred scans. In all spectra presented in the results section, spectral subtraction was used to remove background vibration bands of pyrite particles without preconditioning. This allows a better view of the bands corresponding to the species attached to or detached from the pyrite surface as the result of mineral suspension in different aqueous media (see Figures 8–10 below).

Evidence on the pyrite attack by the different liquid media used in the present work were obtained by three techniques. First, BET technique was used to measure the more than a 4-fold increase of the specific surface area of pyrite previously suspended in Na^+-acetate and then dried. Second, qualitative observations of the presence of both Fe and S in supernatants resulting from the pyrite dissolution by deionized water were made with proton-induced X-ray emission (PIXE) technique. This assemblage uses a proton beam generated by a 1.7 MV Pelletron from the National Electrostatic Corporation (Middleton, WI). Third, quantitative Fe determinations in supernatants obtained from assays of pyrite dissolution by aqueous media were done by the phenanthroline-citrate colorimetric technique (Yamamura and Sikes, 1966). Briefly, samples of pyrite (100 mg) were suspended in 2 ml of deionized water or artificial seawater at 45 °C. After 20 min a first set of supernatants were removed by centrifugation for the Fe determinations. A second set of supernatants was prepared using the sediments from the first set in 2 ml of identical fresh solutions, incubated again for 40 min. Both the former and latter supernatants were mixed with the 1,10-phenantroline reagent to measure iron in solution as referred above.

3. Results

The main purpose of this study was the monitoring of both P_i attachment onto the pyrite interface and its modulation by specific modifications of the aqueous media. The main medium was artificial seawater (Snyder and Fox, 1975) simulating primeval scenarios in the cooler vicinity of the main hot vents (Corliss, 1990; Ozawa *et al.*, 2004). Modifications of the electrolyte species and concentration can affect sorption processes, and they were identified with the variation of artificial-seawater composition, pH, or the incubation conditions.

The high SO_4^{2-} concentrations used in some of the assays discussed were needed in order to highlight the attenuation of the P_i sorption in the presence of this anion (Figure 6) and its effect on the surface charge of pyrite particles (Figures 7 (B and C). In particular, in the case of these electrophoretic determinations the SO_4^{2-} concentrations used are required to clearly evaluate the SO_4^{2-} induced charge modification of pyrite grains of about 50 μm. The chosen high phosphate concentration used in most of the assays (0.6 mM P_i) had also the same purpose of demonstrating specific P_i sorption/desorption properties.

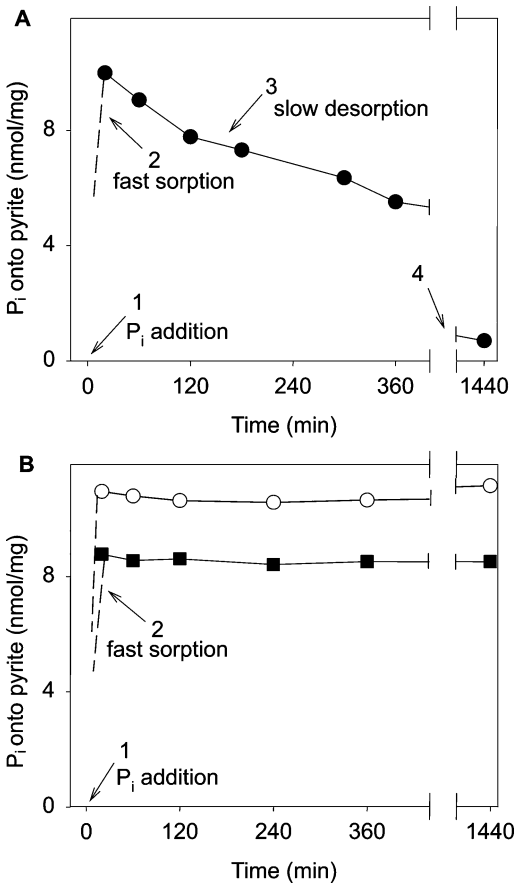

Fig. 1 Time course of P_i sorption onto pyrite. (A): At zero time (arrow 1) samples containing 50 mg pyrite were suspended in 1 ml of artificial seawater with 0.6 mM P_i. (B): Samples with the same amount of pyrite suspended in 0.2 M Na^+-acetate plus 75 mM $MgCl_2$ (◯), or deionized water (■) and supplemented with 0.6 mM P_i at zero time (arrow 1). In all conditions, the initial, fast raising phase of sorption (dashed lines and arrow 2) cannot be time resolved by the separation method employed. One should note the slow desorption taking place with seawater (arrow 3). Arrow 4 points up the level that it is achieved in 24 h by this slow desorption process. The P_i sorbed onto the pyrite crystals was measured at the times shown on the abscissa, using the procedure described in Materials and Methods. All samples were incubated in O_2-free atmosphere at 45 °C

Figure 1A shows the time course of P_i sorption onto pyrite suspended in artificial seawater under an inert argon atmosphere. Figure 1B shows the time courses obtained with Na^+-acetate plus $MgCl_2$ (◯) and deionized water (■). The data of the initial fast raising phase could not be obtained with the separation method employed. For artificial seawater (Figure 1A) there is a slow but progressive decrease of the amounts of sorbed P_i after the initial fast and near complete sorption phase. For the other two aqueous media of Figure 1B, P_i sorption reaches a plateau within 20 min and its liberation phase is absent. This plateau could be ascribed to either the formation of a P_i outer-sphere complex at the pyrite-solution interface or to a direct monodentate binding (Pontes-Buarque *et al.*, 2001, and references therein). The unexpected trend observed with artificial seawater (Figure 1A) reveals that the P_i release might be due to pyrite dissolution. This point will be later considered in more detail.

Figure 2 presents the time-course results obtained after conditioning pyrite samples for 20 min incubation periods and then centrifugated under an O_2-free atmosphere to separate the solid and the aqueous phases. The sediments were then immediately resuspended in the aqueous solutions described in the legend. Contrasting with the data of Figure 1A, one should emphasize that Figure 2A shows no release of sorbed P_i when the pyrite particles are resuspended in three different aqueous media in the absence of P_i: artificial seawater (■); 0.2 M Na^+-acetate plus 75 mM $MgCl_2$ (◯); and deionized water (▲).

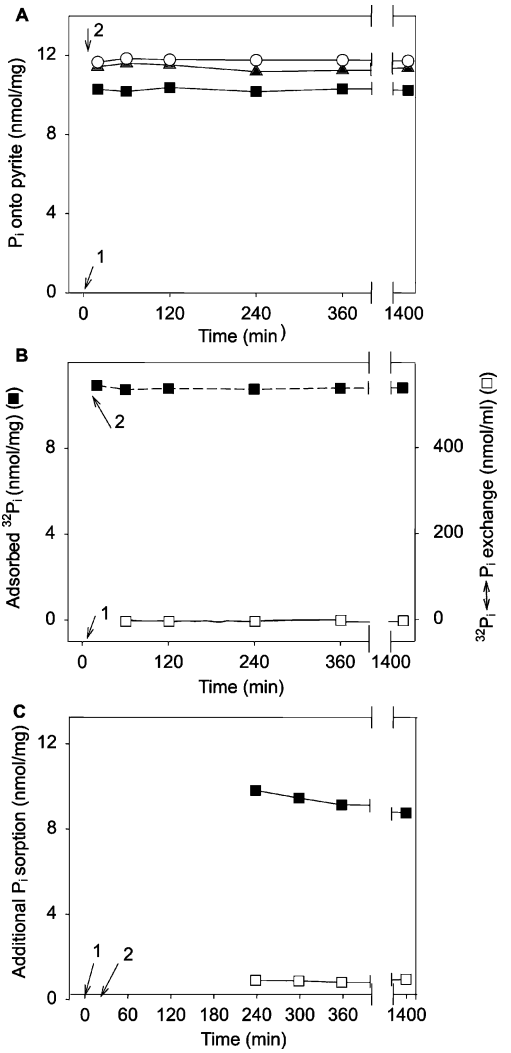

Fig. 2 (A): Residual P_i immobilized by pyrite after removal of the initial suspending aqueous phase. At zero time (arrow 1), samples containing 50 mg of pyrite were suspended in artificial seawater (■), 0.2 M Na^+-acetate plus 75 mM $MgCl_2$ (◯), or deionized water (▲), and immediately supplied with 0.6 mM *Pi*. After 20 min, the sediments were separated by centrifugation and resuspended with 1 ml of a solvent identical to the original one but without P_i (arrow 2). The suspensions were incubated again and assayed for remaining sorption of P_i at the times shown on the abscissa. (B): Absence of $^{32}P_i \leftrightarrow P_i$ exchange onto the pyrite surface. Samples containing 50 mg of pyrite were suspended in 1 ml of artificial seawater plus 0.6 mM $^{32}P_i$ (arrow 1). Sorption of $^{32}P_i$ onto pyrite was measured after 20 min. At this time (arrow 2) the supernatants of the samples were removed by centrifugation and the sediments resuspended in 1 ml of fresh artificial seawater containing 0.6 mM of unlabeled P_i. The release of $^{32}P_i$ from pyrite (exchanged with unlabeled P_i in nmol/ml of medium; □) and the remaining sorbed $^{32}P_i$ (■) were assayed at the times shown in the abscissa. (C): Additional sorption of P_i onto pyrite after a first cycle of sorption followed by removal of the supernatant. At zero time (arrow 1) samples containing 50 mg of pyrite were resuspended in 1 ml of artificial seawater plus 0.6 mM P_i. After 20 min, the samples were centrifuged, the supernatants were discarded and the P_i-loaded pyrite sediments were resuspended (arrow 2) with 1 ml of fresh seawater plus 0.1 mM (□) or 0.6 mM (■) of P_i and incubated again in the same conditions. Ordinate shows additional sorption of P_i at the instants of time shown on the abscissa (i.e. sorption of new P_i onto previously P_i-coated pyrite)

Table 2 Absence of $^{32}P_{i(s)} \leftrightarrow P_{i(aq)}$ exchange after chase of pyrite samples with seawater containing large amounts of unlabeled P_i [a]

$^{32}P_i$ used in sorption (mM)	Unlabeled P_i used in chase (mM)	Time after chase (h)	Remaining sorbed $^{32}P_{i(\%)}$
0.6	6	1	99.3
0.6	6	24	99.3
0.6	10	1	98.6
0.6	10	24	98.6

[a]After sorption of $^{32}P_i$ for 20 min the supernatants were removed and the sediments were resuspended in artificial seawater containing the unlabeled P_i concentrations shown in column 2. The remaining percent amounts of sorbed $^{32}P_i$ after the incubation times shown in column 3 are given in column 4.

When P_i is present in the new suspension with artificial seawater — after the preconditioning described for Figure 2A – no exchange between sorbed and medium P_i is observed within the resolution of the present observations, even for high P_i concentrations, provided that the first aqueous phase is removed after centrifugation and replaced by a fresh one. Table 2 shows the relative amounts of remaining sorbed $^{32}P_i$ onto pyrite after resuspensions for 1 h and 24 h in artificial seawater containing either 6 mM or 10 mM unlabeled P_i. Figure 2C shows that the initially sorbed P_i remains bound to pyrite for long periods of time when the initial supernatant was removed and the sediments resuspended with fresh seawater supplied with different P_i concentrations (arrow 2). In this new conditioning, additional surface sites can be permanently occupied by P_i in a concentration-dependent manner contrasting with that observed in Figure 1A after 240 min. The fact that newly added 0.1 and 0.6 mM P_i are almost completely removed from the medium (Figure 2C) by previously P_i-coated pyrite reveals that there exists an excess of P_i-available sites in the amount of the mineral used in the assay.

The desorption effects of different supernatants on initially trapped P_i are shown in Figure 3. For reference, the lower levels of residual P_i on pyrite remaining after 24 h (column A; see also Figure 1A) are not seen anymore (column B) when pyrite particles loaded with P_i are resuspended with a supernatant that was recovered after 24 h of contact with pyrite but in the absence of P_i. However, an unexpected result is found when these same pyrite samples are incubated during 24 h with the 24 h old P_i-containing supernatant used in the assay shown as bar A (column C). The desorption efficiency observed in this last assay indicates that P_i itself can play a significant role on its own release from pyrite in combination with the species found in the first supernatant (Table 3). This point will be discussed below.

Assays to determine the presence of both sulphur and iron due to pyrite dissolution by water were made by the PIXE method. The supernatants were obtained with incubation periods within 24 h of 50 mg of pyrite particles suspended in 1 ml of deionized water. The PIXE data – not shown – confirmed the expected presence of these elements in the supernatants due to pyrite dissolution. Quantitative results concerning iron release are shown in Figure 4. It is clearly observed in this figure that iron release in seawater is more effective than that observed for deionized water, the initial release being twice that observed for P_i in the former medium – an observation that gives support to the expectation that P_i release is promoted by pyrite dissolution. Figure 4 also shows that a marked dissolution is only present in the seawater assay of the first 20-min incubation, before removal of the initial supernatant (column A). Iron release becomes similarly low for both artificial seawater and

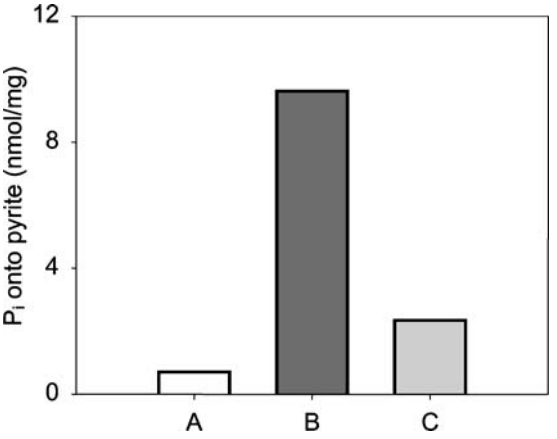

Fig. 3 Role of the starting supernatant and of P_i in the desorption of previously sorbed P_i. Pyrite samples (50 mg/ml) were incubated in artificial seawater supplied with 0.6 mM P_i. After 24 h, their sorption levels were measured (A) and the supernatants were kept under argon atmosphere. A second set of pyrite samples were incubated for 20 min in artificial seawater containing 0.6 mM P_i, the supernatants were removed and discarded, and the sediments were resuspended with the supernatants of pyrite samples incubated in artificial seawater for 24 h as in (A) but without P_i. The remaining sorbed P_i was measured after a new incubation period of 24 h (B). In a third experiment the same P_i-containing sediments used in assay (B) were resuspended in 1 ml of the supernatants obtained from the assay (A) and incubated during 24 h. The remaining levels of adsorbed P_i are shown in (C)

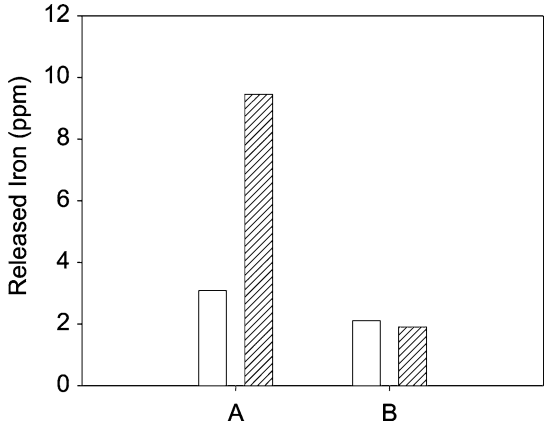

Fig. 4 Iron release from pyrite samples incubated with P_i in either deionized water (empty bars) or artificial seawater (shaded bars). Pyrite samples (50 ml/ml) were suspended during 20 min (A) and the supernatants were removed by centrifugation and assayed for free iron. Assays (B) show the iron release from pyrite samples after removal of the 20 min supernatant followed by resuspension of the sediments in fresh seawater supplied with P_i

deionized water after the removal of the first supernatant and resuspension with fresh solutions (column B).

Figure 5 shows pH effects on the time course of P_i sorption onto pyrite dispersed in seawater. As in the above results, the curves shown in this figure exhibit the same biphasic character with an initial fast sorption phase that is not time resolved (arrow). The second phases of these curves, however, exhibit different behavior. It can be observed that the more acidic medium (pH 4.0) favors P_i-immobilization, supporting the supposition that soluble P_i was absent in the acidic Hadean ocean. The assays with pH 5.5 reproduces the trend observed in Figure 1 – the gradual release of sorbed P_i – which becomes more pronounced with mildly alkaline medium (pH 6.6). Besides the pH influence, medium vi-

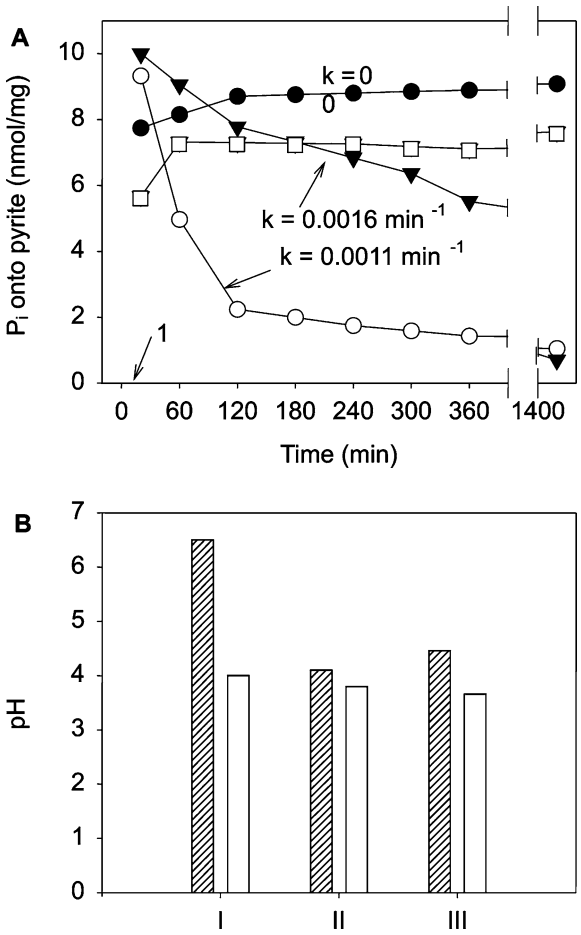

Fig. 5 (A): P_i sorption and desorption in acidic or mildly alkaline seawater. Pyrite samples (50 mg) were suspended (arrow 1) in 1 ml of artificial seawater at initial pH values 6.6 (◯), 5.5 (▼) or 4.0 (●). The desorption rate constants (k) were calculated using single exponentials. The assay at pH 6.6 was repeated (□) with vibrating suspension (80 cycles/min). The fast raising sorption phase cannot be resolved within the time resolution of the experiments. (B): Time course of the suspension pH for different starting values. Pyrite samples were incubated in P_i-free artificial seawater at initial pH values of 6.5 (shaded columns) or 4.0 (empty columns) in assays labelled as (I). After 20 min, the supernatants were removed and replaced by fresh solutions without P_i (assays II) or with 0.6 mM P_i (assays III). The pH values remained constant throughout the assayś duration (24 h)

bration should be also considered in the P_i release from an outer sphere and, for this reason, sorption data obtained at pH 6.6 under agitation are also shown in Figure 5. Once again, the suspension vibration induces P_i resorption, reproducing the results presented in Figure 1B. The major conclusion from this set of assays is that the survival rate of soluble P_i should increase in alkaline seawater. This point will be especially discussed below.

The above results suggest that changes in the salt composition of the artificial seawater might affect P_i immobilization by the interface of a mineral and surrounding aqueous environment (Figures 1, 2, and 5), for, as shown in Figure 6, solutions with different salts have specific effects upon this immobilization. As it can be seen in Figure 6A, the removal of either the prevailing monovalent cations in seawater, Na^+ and K^+ (I), or of the divalent Mg^{2+} (II) strongly attenuates the otherwise fast P_i sorption component shown in Figures 1 and 2 – an effect that can be attributed to a decrease of the positive bridging charges within the interface.

Three possible sources of SO_4^{2-} in primitive aqueous niches were considered for the assays with this anion: (1) crustal emissions of highly soluble sulfur gases into the primordial Earth atmosphere would be trapped in the Hadean seas, mostly in the form of SO_2.

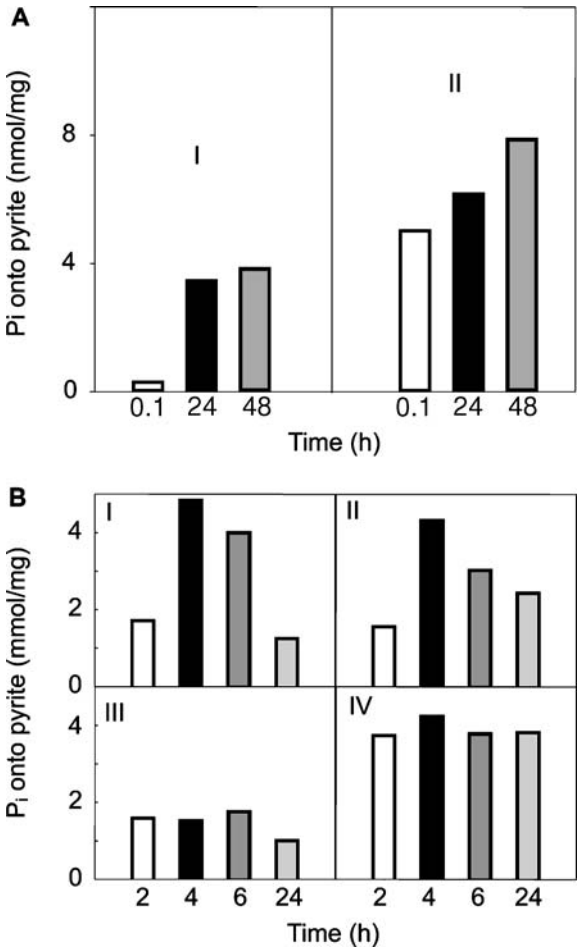

Fig. 6 Time courses of P_i sorption identifying electrolyte effects. (A): Pyrite samples (50 mg) suspended in the following 1 ml solutions containing 0.6 mM P_i: artificial seawater without both NaCl and KCl (I) or artificial seawater without $MgSO_4$ (II). (B): Pyrite samples (50 mg) suspended in the following 1 ml solutions containing 0.6 mM P_i: 0.5 M Na_2SO_4 plus 0.5 M $MgSO_4$ (I); 0.5 M Na_2SO_4 (II); 0.5 M $MgSO_4$ (III); or 0.5 M $MgCl_2$ plus 0.5 M NaCl (IV). At the times indicated in the abscissa the samples used for the results shown in both A and B were centrifuged and the supernatants removed to measure the sorbed P_i

The subsequent formation of sulfite and bisulfite as intermediary species would evolve into sulfate and sulfide at some indeterminate rate (Schlesinger, 1997; Kasting, private communication, 2006); (2) the dissolution of anhydrite ($CaSO_4$) due to cold seawater flows through hydrothermal vent systems (Pilson, 1998); (3) SO_4^{2-} as the product of the oxidation of pyrite due to its interaction with water (Borda *et al.*, 2003; Usher *et al.*, 2004). The effect of SO_4^{2-} on P_i sorption has thus been considered in the present work. Figure 6B shows the effect of the SO_4^{2-} anion on P_i sorption for different cation combinations. The comparison of the results lead to the conclusion that SO_4^{2-} decreases P_i sorption and contributes to its release, since: (a) in Na^+-containing media (with 0.5 M SO_4^{2-}) sorption reaches a peak after 2 h instead of 20 min (I) (with 26 mM SO_4^{2-}); (b) the rate of detachment decreases with lower SO_4^{2-} concentration (II); (c) P_i sorption is inhibited with high SO_4^{2-} in the absence of Na^+ (III); and (d) fast, high and stable levels of P_i sorption are found with no SO_4^{2-} in Na^+-containing medium (IV). Taken together, these data clearly indicate that SO_4^{2-} could have played a crucial role in modulating the availability of soluble P_i in special primitive niches. As it can be seen in Figure 7B, this SO_4^{2-} effect is supported by the observed increase of the surface negativity of pyrite particles dispersed in SO_4^{2-}-rich solutions.

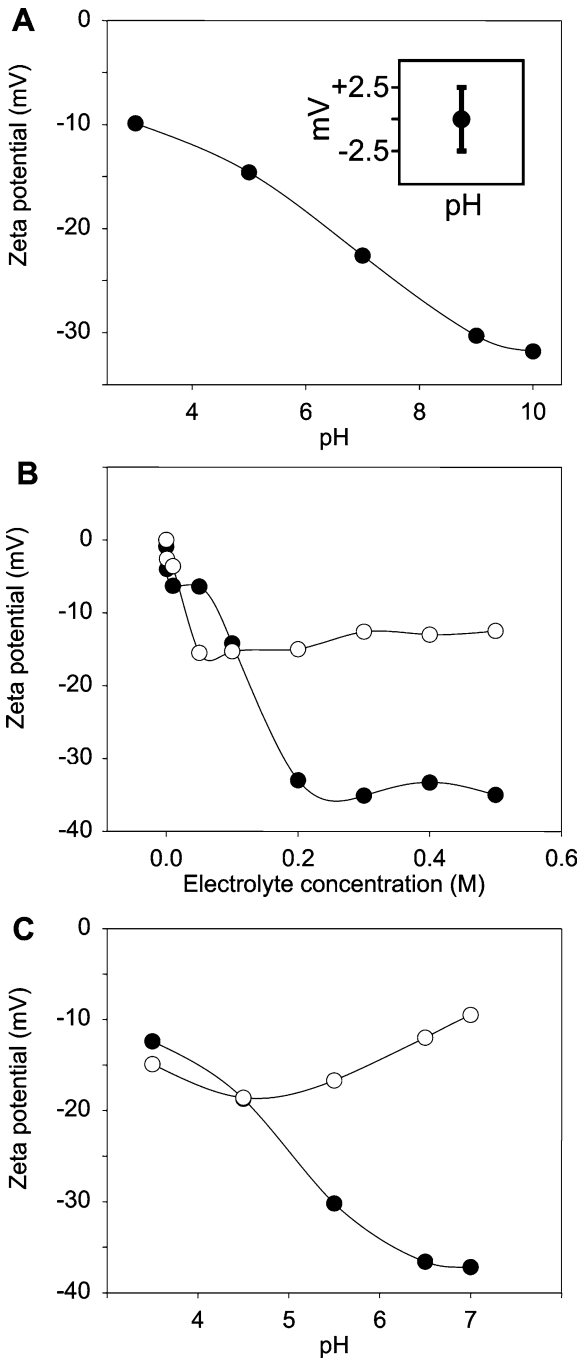

Fig. 7 Zeta potential determinations of surface charge polarities of pyrite particles dispersed in water. The insert shows the uncertainty of these zeta-potential determinations. (A): The pH dependence of the Zeta potential of pyrite particles dispersed in water. (B): The electrolyte dependence of the Zeta potential of pyrite particles in suspensions of water with KCl (◯) and $MgSO_4$ (●), at pH 6.6. C: The pH dependence of the Zeta potential of pyrite particles dispersed in water containing P_i 0.6 mM (◯), or P_i 0.6 mM plus $MgSO_4$ 0.1 M (●)

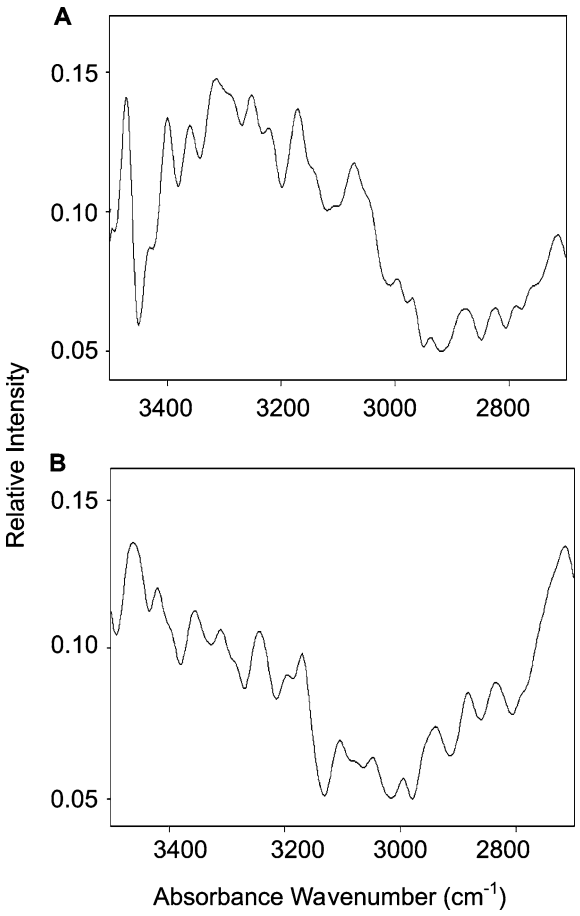

Fig. 8 IR spectra (3500 cm^{-1} ↔ 2700 cm^{-1}) obtained with pyrite samples previously incubated with artificial seawater with 0.6 mM P_i. (A): IR spectrum of samples after 20-min of incubation. (B): IR spectrum obtained after a second incubation as follows. After the initial 20 min incubation, the supernatant was removed and the residual sediment dispersed for another 20 min in fresh artificial seawater with 0.6 mM P_i

Complementary observations of the polarization of the pyrite surface were made by Zeta potential determinations. In these assays, the pyrite particles were dispersed in solutions with specific electrolytes at differing pH values. The results shown in Figure 7A clearly indicate that the negative polarity of pyrite particles increases with pH. This trend confirms the expectation that the observed results obtained with model alkaline seawater (Figure 5A) can be associated with the outer charge polarity of the pyrite interface. As mentioned above, the data shown in Figure 7B demonstrate that SO_4^{2-} concentrations beyond 0.2 M can provoke a marked increase of negative polarity of the particle interface. It can be also inferred from the results of Figures 6A and 7B that the Mg^{2+} ion should be bridging the attachment of the P_i onto the pyrite interface.

Further evidence supporting the view that the interface is modified with the preconditioning in P_i-containing seawater are given in Figures 8 to 10 of the infrared spectra, IR, obtained with pyrite after removal of the supernatants. The full spectra of the different supernatant compositions were not determined experimentally. Thus we surveyed the IR literature for 1650 cm^{-1} bands of viable molecules or ionic structures, *i.e.* the IR vibration centers that could be formed and/or detached during those incubations. Table 3 summarizes the normal vibrations of sulfate and phosphate as well as of the possible species at about 1650 cm^{-1} which

Table 3 Normal vibrations of sulfate and phosphate in infrared spectra

Band	Wavenumber (cm^{-1})	Reference
Sulfate:		
$S{=}0$	1650	Silverstein and Webster, 1998
Sulfate in solution	1100	Borda *et al.*, 2004
Disulphide	440	Evangelou and Huang, 1994
Phosphate:		
Phosphate bands[a]	1200–1100	Persson *et al.*, 1996
Phosphate bands[b]	1100	Persson *et al.*, 1996
Protonated phosphate band ($HPO_{4aq}{}^{2-}$)	1087	Persson *et al.*, 1996
Proposed supernatant species[c]:		
Iron-bond H_2O	1650	Evangelou and Huang, 1994
$CO_3{}^{2-}$ + Fe (II)	1650	Evangelou and Huang, 1994
$CO_3{}^{2-}$ in solution	1650–1350	Vilalobos and Leckie, 2001

[a]Goethite, pH 4.2 → 5.7
[b]Hematite, pH 4.0 → 6.5
[c]Figure 9, this paper

could have been detached from the pyrite during the second incubation. The spectra shown in Figures 8A, 9A and 10A were obtained after conditioning by 20 min incubation, while those shown in Figures 8B, 9B and 10B were obtained after conditioning by two successive 20- min incubations of pyrite particles in artificial seawater with 0.6 mM P_i. The bands in all the Figures 8A, 9A and 10A denote the presence of species formed during the first incubation and, due to its poor solubility, deposited onto the sediment – or formed at the surface itself as in the case of $SO_4^{2-}{}_{ads}$ from OH_{ads} and released sulfur (Borda *et al.*, 2003) – and kept in the sediment after centrifugation. During the second incubation, dilution of these coatings takes place and the corresponding band species became barely detectable. The comparison of the IR data obtained with one or two conditionings reveals significant changes. The band structure shown in the 3200 cm^{-1} region of Figure 8A – which has been identified as that for O-H stretching frequencies for a variety of inorganic minerals (Libowitzky, 1999) – is significantly reduced after incubation stages (Figure 8B). The broad band seen at 1650 cm^{-1} after 20 min incubation (Figure 9A) is again greatly reduced after the second incubation treatment (Figure 9B). In connection with the observations of Figures 7B and 7C, it is important to mention that a $S=O$ vibration band – evidently coming from a complex attached to the interface – is known to exist in this region (Silverstein and Webster, 1998), and it also becomes attenuated after removal of the second supernatant. Finally, the main band structure seen in Figure 10 deserves special mention. It is known that sorbed SO_4^{2-} onto pyrite is reported by Evangelou and Huang (1994) to have a signature contribution in the 1100 cm^{-1} region and it also decreases after replacement of the first supernatant. Moreover, the shoulder denoted by an arrow in Figure 10B, that can be assigned to PO_4 vibrations (see Table 3), is in agreement with the proposal that P_i remains bound to the interface, as directly shown with the results previously described in the Figure 2A.

4. Discussion

Most of the above results are relevant for the hypothesis of early molecular evolution on the surface of sulfide minerals leading to the advent of life, and they are consistent with

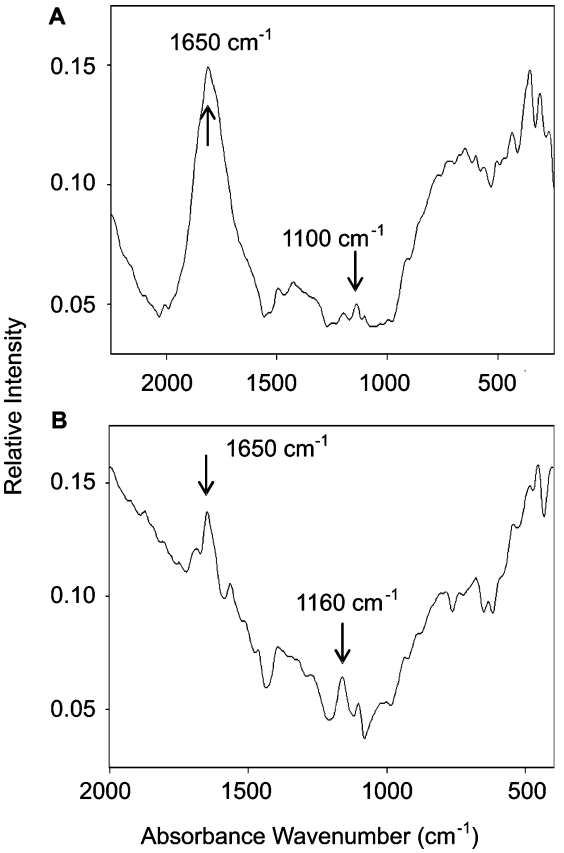

Fig. 9 IR spectra (2000 cm^{-1} ↔ 400 cm^{-1}) obtained with pyrite particles previously incubated with artificial seawater with 0.6 mM P_i. The data shown in both A and B were obtained using the procedures described in the legend to Figure 8

the present knowledge of reactive pyrite (Schoonen *et al.*, 2000). The slow release of P_i after its efficient and fast sorption (Figure 1A) is an indication that a gradual dissolution of pyrite takes place (Paschka and Dzombak, 2004). This is consistent with the enhanced iron detachment shown in Figure 4.

Another relevant conclusion of this work also arises from the comparison of Figures 1A and 3 where it is shown that P_i present in artificial seawater can induce its detachment from pyrite and, consequently, its transfer to an homogeneous phase if the initial supernatant is kept. Possibly, a combination of mechanisms could cause the release of P_i in the presence of both the first supernatant and of P_i. The precipitation of the insoluble P_i species formed and released during the first incubation (Table 2; see also Figures 8–10 below) could activate the pyrite dissolution process. Another process could be linked to an enhanced local SO_4^{2-} formation induced by P_i. It is known that the rate of the formation of OH *via* the Fenton reaction increases by more than two orders of magnitude if Fe^{2+} is bound to a low-molecular weight phosphorylated compound (Biaglow *et al.*, 1996). Thus $OH\cdot_{ads}$ plus liberated sulfur (Borda *et al.*, 2003) will lead to the formation of $SO_4^{2-}{}_{ads}$ with concomitant increase in the negativity of the surface. As shown in Figures 7B and C, the SO_4^{2-} coatings increase the negative charge of the surface and this could promote P_i release.

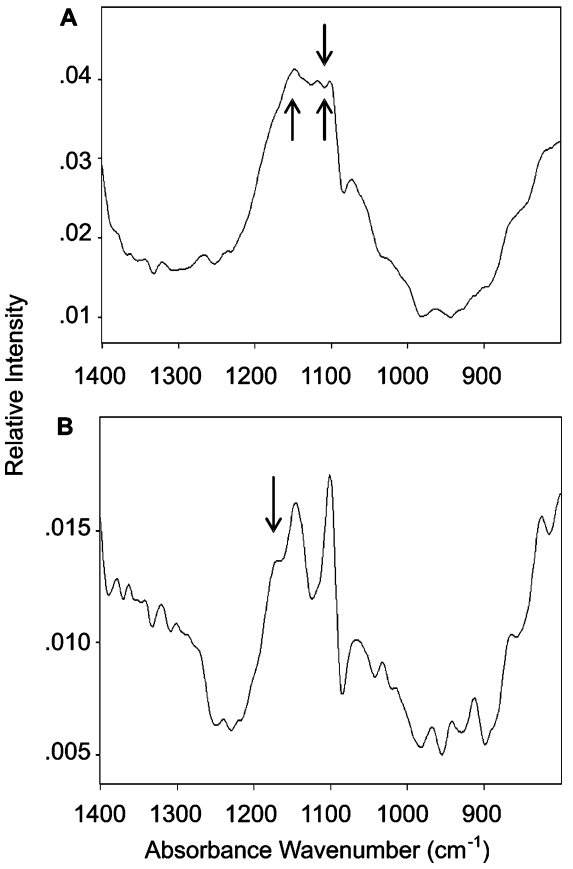

Fig. 10 IR spectra within the range $1400\,cm^{-1} \leftrightarrow 800\,cm^{-1}$. A and B show the details of the $1100\,cm^{-1}$ region in Figure 9

To explain the absence of P_i release from the interface in a medium containing both Na^+-acetate and Mg^{2+} (◯), shown in Figure 1B, one should recall that: (i) SO_4^{2-} is not present in these assays; (ii) hydrophobic acetate-coating (Pontes-Buarque *et al.*, 2001) could block the detachment mechanisms proposed above; (iii) the increase in the specific surface area measured by BET technique after suspension in acetate (see Materials and Methods section) would provide additional hydrophobic reactive pyrite sites. The efficient P_i attachment observed in Figure 1B with deionized water (■) is apparently a surprising result. However, one should note that: (i) once again SO_4^{2-} is not present; (ii) iron detachment in deionized water is three times smaller than that that it is observed with seawater (Figure 4); and (iii) P_i is known to reduce pyrite oxidation and formation of SO_4^{2-} in pure water (Nyavor and Egiebor, 1995). Thus, the observed efficient and stable attachment in deionized water reveals that, in this less aggressive medium, P_i itself can help to avoid pyrite dissolution and its own release from the interface.

In order to discuss the P_i sorption trends presented in Figures 2A, 2B and 2C, one should review the IR results of Figures 8 to 10 (see also Table 3). The assumptions that are consistent with these IR data are as follows: (i) outer-sphere SO_4^{2-} complexes can be diluted and removed by the second suspending medium after stirring and centrifugation of the first conditioning stage (see the intensity decrease of the band structure at $1650\,cm^{-1}$ (Figure 9) and $1100\,cm^{-1}$ (Figure 10); and (ii) the band-structure depletion observed at the IR spectral region beyond

$3200\,cm^{-1}$ (Figure 8) suggests that OH-bonded complexes corresponding to a variety of compounds (except P_i, Figure 10), could also be detached after the second conditioning step. One can thus infer from the results shown in Figure 2 that a P_i coating of the samples – provided the first supernatant is removed – is again contributing to block pyrite dissolution. This view is reinforced with the fact that in these assays the second incubation is done with a pyrite sediment containing sorbed P_i (Figure 2A). The results of Figures 2B and 2C reinforce this conclusion.

The expected competition of P_i for the available Fe-site bonds of the pyrite surface can be readily used to explain the marked changes of P_i sorption observed as the medium becomes mildly alkaline (Figure 5A) due to surface charge modifications (Figure 7A). The presence of SO_4^{2-} in the interface (Figure 7B) – when $MgSO_4$ is in the medium (Figure 6) – also induces a severe attenuation of the P_i sorption, adding further support to the hypothesis that SO_4^{2-} would have modulated the availability of soluble P_i in specific primeval scenarios. As mentioned above, three processes can be considered for the formation of SO_4^{2-} in these scenarios: SO_4^{2-} formation in condensed seas of the early Earth (Schlesinger, 1997); SO_4^{2-} as the product of water oxidation of the disulfide group (Borda *et al.*, 2003; Usher *et al.*, 2004); and solubilized SO_4^{2-} in cooler seawater flowing through hydrothermal vents systems (Pilson, 1998). Therefore, it is reasonable to propose that SO_4^{2-}, as well as H^+, have been available for modulating mechanisms of sorption/desorption of P_i in microenvironments of the Hadean sea.

5. Conclusions: Possible implications for prebiotic chemistry

It is proposed that alterations of the aqueous solutions, and of the mineral interface itself, could have triggered specific mechanisms of sorption and release of either organic or inorganic molecules in primitive aqueous environments (Lahav *et al.*, 1994). The release of P_i from the interface between iron-sulphur minerals and seawater would have been a convenient source of soluble phosphate for prebiotic reactions either in homogeneous conditions or on the surface of others minerals with adsorptive or catalytic properties. Moreover, the availability of interfacial soluble P_i would also favour early synthesis of mononucleotides in specific aqueous conditions (Pontes-Buarque *et al.*, 2001).

Taken altogether, the results described in this work open up the possibility that pH alkalinization and increase in SO_4^{2-} concentrations in specific niches could have provoked the release of inorganic phosphate compounds from sulphide minerals in primitive microenvironments of the Hadean sea. Released P_i and P_2O_7 anions – which were probably originated in volcanic activity (Yamagata *et al.*, 1991) – would be efficiently adsorbed on surfaces of pyrite structures in cooler regions of a proposed acidic ocean (Martin and Russell, 2002). Alkaline vent emissions in these surroundings would promote the release of P_i making it available in soluble form at milder temperatures. The relevance of the proposed mechanisms of P_i capture, release and trapping arises from the need of abundant presence of this molecule for primitive phosphorylations. Similarly to contemporary aqueous media average P_i presence in primitive seas should have been too sparse (Keefe and Miller, 1995); however, in the hydrothermal scenarios considered in this work, condensation of phosphate species might produce concentrations in the millimolar range (Arrhenius *et al.*, 1997). Pyrite formations are common features at hydrothermal sites (Shock, 1992), and estimates support the expectations that large volumes of sea water with dilute inorganic molecules – including phosphate compounds – circulate over many times within the geologic time scale through networks of hydrothermal vents (Pilson, 1998). Thus, P_i dispersed in seawater would be exposed to

pyrite formations of these networks; a mineral with strong affinity for reactive P_i (Bebié and Schoonen, 1999; Monte *et al.*, 2003).

As pointed out above, when pyrite decomposition occurs in media with high salinity, previously attached P_i becomes available for phosphorylations in homogeneous conditions – as early proposed for calcium phosphate minerals (Vieyra *et al.*, 1995). In the prebiotic environments simulated in this paper, P_i liberated from sulfides could also have allowed, for example, the formation of phosphorylated compounds. In this process, the surface mineral itself could have acted as an energy-coupling device, a mechanism of catalysis for further molecular complexification after the advent of membranes and insulated compartments (Koch and Schmidt, 1991).

It has been shown in this work that acidic → alkaline transitions can to be an important factor in the modulation of P_i sorption and release in pyrite/seawater interfaces (Figure 5A). Alkaline fluxes may also have been insulated by membrane formation, as has been suggested to occur in the neighbourhood of vent emissions (Russell *et al.*, 1994; Martin and Russell, 2002). In this environment, the combination of trapped P_i with low H^+ concentration could have favored both the exergonic H^+ fluxes across the membrane and the incorporation of the solubilized P_i in high-energy compounds (Koch and Schmidt, 1991). It can be speculated that the legacy of the mechanisms for P_i sorption and release from pyrite interfaces described in the present work remain in modern living systems. For example, charge separation and proton gradient formation in mitochondria, which are essential for phosphorylation and chemical energy transduction (Mitchell, 1977), could have evolved from similar processes existing onto pyrite surfaces during chemical evolution.

Acknowledgements The authors are thankful to Dr. Stenio Dore de Magalhães, Physics Institute/UFRJ, Rio de Janeiro, for the PIXE observations, and to Ms. Antonieta Middea of CETEM/MCT, for the infrared data, and to Prof. James F. Kasting, for a private communication about the primitive sulfur cycle. They also acknowledge Professor Susana L. de S. Barros for critical reading of the manuscript.

References

Arrhenius G, Sales B, Mojzsis S, Lee T (1997) Entropy and charge in molecular evolution: the case of phosphate. J Theor Biol 187:503–522

Bebié A, Schoonen MA (1999) Pyrite and phosphate in anoxia and an origin-of-life hypothesis. Earth Planet Sci Lett 171:1–5

Biaglow JE, Held KD, Manevich Y, Tuttle S, Kachur A, Uckun F (1996) Role of guanosine triphosphate in ferric ion-linked fenton chemistry. Radiat Res 145:554–62

Borda MJ, Elsetinov AR, Strongin MA, Schoonen MA (2003) A mechanism for the reduction of hydroxyl radical at the surface defect sites on pyrite. Geochim Cosmochim Acta 67:935–939

Borda MJ, Strongin DR, Schoonen MA (2004) A vibrational spectroscopic study of the oxidation of pyrite by molecular oxygen. Geochim. Cosmochim. Acta 68:1007–1813

Brunauer S, Emmett PH, Teller E (1938) Adsorption of gases in multimolecular layers. J Am Chem Soc 60:309–319

Cairns-Smith AG (1982) Genetic takeover and the minerals origins of life. Cambridge University Press London, pp 343

Corliss JB (1990) Hot springs and the origin of life. Nature 347:624

Evangelou VP, Huang X (1994) Infrared spectroscopic evidence of an iron (II) – carbonate complex on the surface of pyrite. Spectrochim Acta 50:1333–1340

Fiske CH, SubbaRow Y (1925) The colorimetric determination of phosphorus. J Biol Chem 66:375–400

Hermes-Lima M, Vieyra A (1992) Pyrophosphate synthesis from phospho(enol)pyruvate catalyzed by precipitated magnesium phosphate with "enzyme-like" activity. J Mol Evol 35:277–285

Huber C, Wächtershäuser G (1997) Activated acetic acid by carbon fixation on (Fe, Ni)S under primordial conditions. Science 276:245–247

Keefe AD, Miller SL (1995) Are polyphosphates or phosphate esters prebiotic agents? J Mol Evol 41:693–702
Kasting JF, Zahnie KJ, Pinto JP, Young AT (1989) Sulfur, ultraviolet radiation, and the early evolution of life. Orig Life Evol Biosph 19:95–108
Koch AL, Schmidt TM (1991) The first cellular bioenergetic process: primitive generation of a proton-motive force. J Mol Evol 33:297–304
Lahav N (1994) Minerals and the origin of life: hypotheses and experiments in heterogeneous chemistry. Het Chem Rev 1:159–179
Libowitzky E (1999), Correlation of O-H stretching frequencies and O-H. . .O hydrogen bond lengths in minerals. Monats Chem 130:1047–1059
Martin W, Russell MJ (2002) On the origins of cells: a hypothesis for the evolutionary transitions from abiotic geochemistry to chemoautotrophic prokaryotes, and from prokaryotes to nucleated cells. Phil Trans R Soc Lond B358:59–85
Miller SL, Parris M (1964) Synthesis of pyrophosphate under primitive Earth conditions. Nature 204:1248–1250
Mitchell P (1977) A commentary on alternative hypotheses of protonic coupling in the membrane systems catalysing oxidative and photosynthetic phosphorylation. FEBS Lett 78:1–20
Monte MB, Lins FF, Oliveira JF (1997) Selective flotation of gold from pyrite under oxidizing conditions. Int J Miner Process 51:255–267
Monte MBM, Duarte AC, Bonapace JAP, do Amaral Jr MR, Vieyra A, de Souza-Barros F (2003) Phosphate immobilisation by oxide precursors: implications on phosphate availability before life on Earth. Orig Life Evol Biosph 33:37–52
Nyavor K, Egiebor NO (1995) Control of pyrite oxidation by phosphate coating. Sci Total Environ 162:225–237
Ozawa K, Nemoto A, Imai EI, Honda H, Hatori K, Matsuno K (2004) Phosphorylation of nucleotide molecules in hydrothermal environments. Orig. Life Evol. Biosph 34:465–471
Paschka MG, Dzombak DA (2004) Use of dissolved sulfur species to measure pyrite dissolution in water at pH 3 and 6. Environ Eng Sci 21:411–420
Pilson MEQ (1998) An introduction to the Chemistry of the Sea, Prentice Hall Upper Saddle River New Jersey, pp. 324–325
Persson P, Nilsson N, Sjöberg S (1996) Structure and bonding of orthophosphate ions at the iron oxide-aqueous interface. J Colloid and Interf Sci 177:263–275
Pontes-Buarque M, Tessis AC, Bonapace JAP, Monte MB de M, de Souza-Barros F, Vieyra AR (2000) Surface charges and interfaces: implications for mineral roles in prebiotic chemistry. An Acad Bras Cien 72:317–322
Pontes-Buarque M, Tessis AC, Lopez GC, Monte MBM, Bonapace JAP, Vieyra A, de Souza-Barros F (2001) Modulation of adenosine 5′-monophosphate adsorption onto aqueous resident pyrite: potential mechanisms for prebiotic reactions. Orig Life Evol Biosph 31:343–362
Russell MJ, Daniel RM, Hall AJ, Sherringham JA (1994) A hydrothermally precipitated catalytic iron sulphide membrane as a first step toward life. J Mol Evol 39:231–243
Silverstein RM, Webster FX (1998) Spectrometric identification of organic compounds. John Wiley & Sons New York, 6th Edition, p 140
Schlesinger WH (1997) Biogeochemistry an analysis of global change, Academic Press San Diego, 2nd Edition, p 407
Shock EL (1992) Chemical environments of submarine hydrothermal systems. Orig Life Evol Biosph 22:67–107
Schoonen MA, Elsetinow AR, Borda MA, Stongin DR (2000) Effect of temperature and illumination on pyrite oxidation between pH 2 and 6. Geochem Trans 4:23–33
Snyder WD, Fox SW (1975) A model for the origin of stable protocells in a primitive alkaline ocean. BioSystems 7:222–229
Tessis AC, Amorim HS de A, de Souza-Barros F, Farina M, Vieyra A (1995) Adsorption of 5′-AMP and catalitic synthesis of 5′-ADP onto phosphate surfaces: correlation to solid matrix structures. Orig Life Evol Biosph 25:351–373
Tessis AC, Penteado-Fava A, Pontes-Buarque M, Amorim HS de, Bonapace JAP, de Souza-Barros F, Vieyra A (1999) Pyrite suspended in artificial sea water catalyzes hydrolysis of adsorbed ATP: enhancing effect of acetate. Orig Life Evol Biosph 29:361–374
Usher CR, Cleveland Jr CA, Strongin DR, Schoonen MA (2004) Origin of oxygen in sulfate during pyrite oxidation with water and dissolved oxygen: an *in situ* horizontal attenuated total reflectance infrared spectroscopy isotope study. Environ Sci Technol 38:5604–5606
Vieyra A, Gueiros-Filho F, Meyer-Fernandes JR, Costa-Sarmento G, de Souza-Barros F (1995) Reactions involving carbamyl phosphate in the presence of precipitated calcium phosphate with formation of

pyrophosphate: a model for primitive energy-conservation pathways. Orig Life Evol Biosph 25:335–350

Vilalobos M, Leckie JO (2001) Surface complexation modeling and FTIR study of carbonate adsorption to goethite. J Colloid Interf Sci 235:15–32

Yamagata Y, Watanabe H, Saitoh M, Namba T (1991) Volcanic production of polyphosphates and its relevance to prebiotic evolution. Nature 352:516–519

Yamamura SS, Sikes JH (1966) Use of Citrate-EDTA masking for selective determination of Iron with 1,10-Phenanthroline. Anal Chem 38:793–795